

Facile encapsulation of nanoparticles in nanoorganized bio-polyelectrolyte microshells

Jingmei Su^a, Xia Tao^{a,*}, Hui Xu^a, Jian-Feng Chen^{b,*}

^a Key Lab for Nanomaterials of the Ministry of Education, BUCT, Beijing 100029, China

^b Research Center of the Ministry of Education for High Gravity Engineering & Technology, BUCT, Beijing 100029, China

Received 17 July 2007; received in revised form 9 October 2007; accepted 2 November 2007

Available online 7 November 2007

Abstract

We present a facile method for the encapsulation of nanoparticles' (NPs) systems within the interior space of bio-polyelectrolyte microshells. The microshells, constructed by alternate adsorption of alginate sodium (ALG) and chitosan (CHI) onto the surface of colloidal templates and subsequent removal of cores, allow the polystyrene (PS) or SiO₂ nanoparticles (NPs) adsorbed into the internal shells through a simple mix process, as confirmed by confocal laser scanning microscopy (CLSM), and scanning electron microscopy (SEM) analysis. The NPs-filled microshells form the rigid spherical shape in contrast to the flat and folded structure of microshells at the dry state prior to filling. The interior of NPs-encapsulated microshells was directly visualized by transmission electron microscopy (TEM) image of microtomed slices and cross-section SEM image. The loading amount of NPs in a shell composed of (ALG/CHI)₅ was determined in two media i.e. H₂O and 0.1 M NaCl, and the results showed that the loading amount of the former is greater than that of the latter. The possible encapsulation mechanism is also discussed. The hybrid materials with NPs core and bio-polyelectrolyte shells have potential application for controlled-release drug delivery and catalysis.

© 2007 Elsevier Ltd. All rights reserved.

Keywords: Encapsulation; Microshells; Nanoparticles

1. Introduction

The layer-by-layer (LbL) self-assembly technique firstly introduced by Iler in the sixties has been widely applied to fabricate multilayer ultrathin organic or hybrid films with tailored architecture and properties [1–4]. Recently, the technique has been well developed for the creation of novel microshells with defined internal volume and customized physicochemical properties [5–7]. The fabricated three-dimensional shells, produced by the LbL adsorption of polyanions and polycations onto the surface of colloidal templates and subsequent removal of templates, possess several features including the tailored wall thickness on a nanoscale range, the ordered wall composition,

as well as the controlled size and shape, and hence leading to be potentially applicable as new soft-shell cages in areas such as drug delivery, biosensor, enzyme protection, micro-reactor and catalysis [8,9].

Considerable efforts have been devoted to the nanoscale encapsulation of various species in preformed microshells adjustable to the specific application. The assembled hollow shells composed of synthetic polyelectrolytes such as poly(allyamine hydrochloride) (PAH) and poly(styrene sulfonate) (PSS) or poly(diallyldimethylammonium chloride) (PDDA) and PSS, have been filled with low molecular weight dyes or macromolecules such as PSS, PAH, enzyme and high molecular weight molecules like dextran by changing the permeability of hollow shells via altering the bulk pH values or salt concentrations [10]. Recently, Gao et al. reported a successful encapsulation of macromolecules with ultrahigh molecular weight, for example dextran 2000 kD into PSS/PDDA microshells by means of utilizing the swelling–shrinking features of

* Corresponding authors. Tel.: +86 10 64448472; fax: +86 10 64434784.

E-mail addresses: taoxia@yahoo.com (X. Tao), chenjf@mail.buct.edu.cn (J.-F. Chen).

PSS/PDDA shells in response to external environment stimuli [11]. However, up to date, a significant challenge still remains in incorporating functional nanoparticle systems into the microshells in a controlled manner, and thus preventing the exploration of the various applications with the formed hybrid and functional structures.

Natural polysaccharides such as chitosan (CHI) and alginate sodium (ALG) have been widely investigated for applications in coating membranes, controlled-release drug delivery and biomaterials owing to their proven biocompatibility and safety [12–15]. CHI is a naturally occurring cationic polymer derived from partially deacetylated chitin, which is extracted and isolated from the abundant shells of crustacean. ALG is an anionic polymer composed of a naturally occurring block copolymer of two monosaccharide units obtained from marine brown seaweed. The ALG/CHI polyelectrolyte complex (PEC) systems are commonly developed as a complex planar membrane and an ALG gel bead coated with CHI, which place some limitations in controlling the membrane thickness on a nanometer scale and characterizing the encapsulating PEC membrane precisely [16,17]. Recently, we have constructed a natural and biocompatible polyelectrolyte microshell by using ALG and CHI as building blocks with the LbL self-assembly technique [18,19]. The fabricated ALG/CHI shells were found to have several intriguing advantages over the conventional polyelectrolyte microshells composed of PSS–PAH or PSS–PDDA, including super mechanical/chemical/thermal stabilities and enhanced structure transformation of shell walls in response to external microenvironment. Moreover, spontaneous depositions of organic substances within ALG/CHI shells, such as polyelectrolyte PSS, doxorubicin, and dye molecules have been achieved so far.

In this paper we describe our new attempts to extend the capability and generality of ALG/CHI shells for the encapsulation of entity NPs. We find that polystyrene (PS) and SiO₂ can be easily loaded in the interior of the ALG/CHI shells by simply mixing a suspension solution of the ALG/CHI shells and a suspension solution of NPs overnight at room temperature. The inner structure and morphology of NPs-filled shells was investigated by CLSM, TEM and SEM measurements. The encapsulation process was also discussed. This study provides a novel facile method for the encapsulation of NPs or macromolecules with large geometric structure in defined bio-polyelectrolyte microshells.

2. Experimental

2.1. Materials

ALG ($M_w = 12,000$ – $80,000$) was obtained from Sigma, Canada. CHI ($M_w = 30,000$) was obtained from Primex Biochemicals, Norway. PSS ($M_w = 70,000$) and PAH ($M_w = 70,000$) were obtained from Aldrich. Melamine formaldehyde (MF) particles with a diameter of $4.89 \pm 0.14 \mu\text{m}$ were purchased from Microparticles GmbH, Germany. Fluorescent-labeled polystyrene (PS, 28 nm in diameter, green fluorescing 1% solid) NPs were purchased from Duke Scientific

Corporation, USA. SiO₂ particles (~ 280 nm) were prepared according to Ref. [20]. Polystyrene particles with a diameter of ca. 260 nm were synthesized by emulsion polymerization. All chemicals were used as-received. Millipore water was used throughout the study.

2.2. Shell fabrication

The method for the shell fabrication is taken from Ref. [18]. Briefly, an alginate solution or a chitosan solution with a charge opposite to that of MF templates or the last layer deposited was added to a template colloidal solution for 1 h, followed by three repeated centrifugation/washing/redispersion cycles with dilute aqueous NaCl. After five dilayers of ALG/CHI were adsorbed, the coated particles were treated in HCl to decompose the MF cores. The produced MF decomposition products and excess HCl were washed off until neutral pH was established by centrifugation and water wash. The outermost layer in this study is always the positively charged CHI. The as-prepared shells are centrifuged, and then re-dispersed in phosphate buffer saline (PBS) solution in stock.

2.3. Entrapment of nanoparticles in shells

Equal amounts of a microshell suspension (aged for appropriate two days) and a nanoparticle suspension were simply mixed together overnight at room temperature to obtain the filled shells.

2.4. Characterization

Field emission scanning electron microscopy (FE-SEM, XL-30 FEI Inc., USA) was utilized to observe the morphologies of hollow shells and NPs-filled shells. FE-SEM images were obtained by drying a drop of dispersion on a sample holder in air at room temperature, followed by sputter coating a thin gold layer on as-prepared specimens. FE-SEM was operated at 15 kV.

To view the interior of the filled shells, the NPs-loaded shells were dried and then embedded in epoxy resins holders. Ultrathin sections (30–100 nm in thickness) were obtained using a Leica ultracut UCT ultramicrotome. Copper grids were used to support the thin sections and a Japan Hitachi H-800 TEM was employed for analysis. The cross-sections of the filled shells were obtained by using a glass cutter to scratch the embedded specimens for further SEM analysis.

Confocal micrographs were taken with an LSM 510 confocal microscopy (Carl Zeiss Inc.) equipped with a 100 \times oil immersion objective with a numerical aperture of 1.4. The microshells in an aqueous environment were visualized by FITC-PS with the excitation wavelength of 488 nm.

3. Results and discussion

Well-constructed ALG/CHI microshells were prepared using a colloidal templating LbL procedure as described in Section 2. Fig. 1(a) gives a SEM image of empty shells

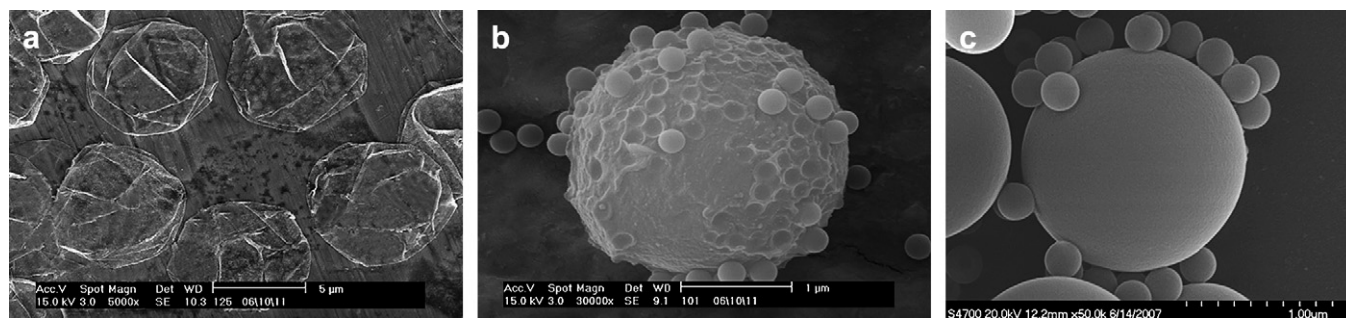


Fig. 1. SEM images of hollow shells of (ALG/CHI)₅ (a), SiO₂-loaded (ALG/CHI)₅ shells (b) and PS-loaded (ALG/CHI)₅ shells (c). The dried hollow shell resembles a deflated balloon. The dried particle-loaded shell looks like a filled balloon.

composed of (ALG/CHI)₅. These thin microspheres adopt folded and deformed morphology on the substrate. The size of the crumpled shells at the dry state is slightly larger than the original MF template size of 4.9 μm , which has also been observed in the polyelectrolyte microspheres of PSS/PAH or PSS/PDDA [21]. After the hollow shells were aged at ambient temperature for two days, a suspension of the (ALG/CHI) shells was mixed with a solution of nanoparticles (NPs) overnight and directly observed under SEM without further separation. Fig. 1(b and c) shows SEM images of NPs-filled (ALG/CHI) shells, in which inorganic SiO₂ and organic polystyrene (PS) NPs were chosen as modeling loading particles. Surprisingly, instead of flat and folded shell structures in SEM images, the mixing process formed rigid sphere aggregations with some nanoparticles sitting on or partially embedded in the main sphere surface. This observation strongly indicated that NPs can migrate across the shell walls and then stay in the interior during the mixing process. It is worth mentioning that the diameter of NPs-loaded shells at the dry state is approximately 2.5 μm for SiO₂ NPs and 1.7 μm for PS NPs, which is significantly smaller than the original template size of 4.9 μm . Meanwhile, the NPs-filled shells, even if at the dry state, still maintain spherical shape integrated. All these observations suggest that the ALG/CHI shells just like an elastomer possess strong mechanical property.

The filled shells can be obtained by centrifuge, to remove superfluous NPs present in the suspension solution. To gain direct insight into the filled shell interior, the NPs-loaded shells were embedded in epoxy resin and then treated with an ultramicrotome to obtain ultrathin sections or a glass cutter

to obtain cross-sections for further analysis. Fig. 2(a) presents a TEM image of ultramicrotomed SiO₂-loaded shells.

In this image SiO₂ particles with a size of ca. 280 nm are seen as dark areas; bright areas in the interior of the shells are originated from drop-off of some SiO₂ particles in preparing the ultrathin slice sample. TEM analysis confirms that SiO₂ NPs are mainly entrapped in the inner space of the shells. Although the outer profile of the NPs-encapsulated shells is discerned as a spherical shape as a whole, the structure of shell walls is difficult to perceive owing to low contrast of organic materials i.e. the shells (ALG & CHI) and the embedding materials (epoxy resin used here). Fig. 2(b) shows a cross-section SEM image for SiO₂-loaded shells. Evidently, SiO₂ NPs indeed enter into the (ALG/CHI) shell interior and the spherical profile of NPs-loaded shells, which is in agreement with TEM image of ultramicrotomed slice (Fig. 2(a)), was also observed.

The amount of unencapsulated NPs remaining in the supernatant liquid was estimated by centrifuging, drying and weighing up. Thus, the loading amount of NPs into the shells was obtained by the difference between the initial amount of NPs latex added and the amount of unloaded NPs from the supernatant liquid. We made a comparison for the encapsulation of particles in different media such as H₂O and NaCl, in which the encapsulation amount may be expressed with weights of particles per shell. The loading result is shown in Table 1. In pure water, the encapsulated amount for the SiO₂ NPs is 6.0×10^{-3} $\mu\text{g}/\text{shell}$, and for the PS NPs, the encapsulated amount is 0.8×10^{-3} $\mu\text{g}/\text{shell}$. Whereas in NaCl media, the encapsulated amount is 3.5×10^{-3} $\mu\text{g}/\text{shell}$ for SiO₂ NPs

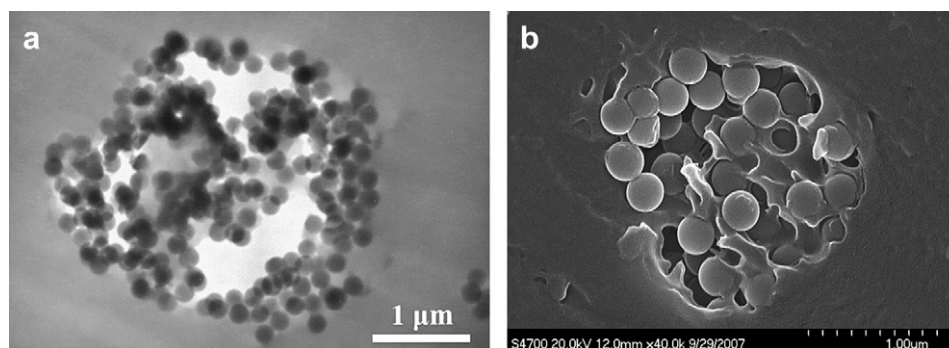


Fig. 2. (a) TEM image of ultramicrotomed slice for NPs-loaded ALG/CHI shells; (b) cross-section SEM image for NPs-loaded ALG/CHI shells.

Table 1
Loading behavior of nanoparticles (NPs) in the hollow (ALG/CHI)₅ shells^a

NPs	Pure water		NaCl solution (0.1 M)	
	SiO ₂	PS	SiO ₂	PS
Size	280 ± 76	260 ± 12	280 ± 76	260 ± 12
Concentration of NPs [mg/ml]	100	10	100	10
Amount of NPs added ^b [mg]	7.1 × 5	1.2 × 5	7.1 × 5	1.2 × 5
Loading amount of NPs [$\times 10^{-3}$ g shell ⁻¹]	6.0 ± 0.2	0.8 ± 0.07	3.6 ± 0.1	0.5 ± 0.05

^a In each experiment, 30 mg of MF particles were used to fabricate (ALG/CHI)₅ shells, which corresponds to ~ 0.5 million of preformed shells. The amount of unencapsulated NPs remaining in the supernatant liquid was estimated by centrifuging, drying and weighing up. Thus, the loading amount of NPs into the shells was obtained by the difference between the initial amount of NPs latex added and the amount of unloaded NPs from the supernatant liquid.

^b To calculate the encapsulating amount of NPs in the shells, unencapsulated NPs in five Eppendorf tubes were collected together, dried, weighed up, and finally give an average result for two independent experiments.

and 0.5×10^{-3} $\mu\text{g}/\text{shell}$ for PS NPs. Apparently, the loading amount in H₂O is greater than that in NaCl. It is understandable because the addition of Na⁺ ions can enhance the electrostatic interaction of the network structure composed of ALG and CHI, which will inevitably arise the decrease of the permeability of the shell walls, and hence at last leads to the reduction of the loading amount [16]. Besides, from Table 1, one can also see that the loading amount of NPs in the shells is proportional to the initial concentration of the NPs added, and hence leads to the SiO₂ NPs-loaded shells (2.5 μm , in size) at the dry state greater than PS NPs-loaded shells (1.7 μm , in size) though the size of SiO₂ NPs and PS NPs is similar.

In order to further clarify special encapsulation capability of the (ALG/CHI) shells, we carried out the comparison experiments on encapsulating NPs into the ALG/CHI, PSS/PAH or PSS/PAH/ALG/PAH shells by CLSM observations, in which FITC-labeled PS NPs with a diameter of ca. 28 nm was chosen as the loading NPs. As shown in Fig. 3, more intense green fluorescence was observed from shell interior rather than

from the bulk when a suspension of the ALG/CHI shells was mixed with a solution of FITC-labeled PS NPs (for interpretation of the references to colour in this figure, the reader is referred to the web version of this article). This result clearly demonstrates that PS NPs can migrate across the layer wall and enter into the shells without any means of assistance. Concomitantly, the colour of the mix solution changed from the initial yellow-green to yellowish, also suggesting that the successful entrapment of FITC-labeled PS NPs inside the shells. In addition, we carried out the encapsulation of fluorescent-labeled PS NPs in the (ALG/CHI)₃ or (ALG/CHI)₄ shells, and found that PS NPs are also loaded in the interior of the shells effectively by CLSM measurements except that the profile of the loaded (ALG/CHI)₃ shells is not very clear. For all PS NPs-loaded shells no deformation or rupture was observed. For the PSS/PAH or PSS/PAH/ALG/PAH shells, one can see that FITC-labeled PS NPs were mainly concentrated on the peripheral rings instead of the interior of the shells (Fig. 4). The diameter of the (PSS/PAH)₅ or (PSS/PAH)/(ALG/PAH)₄ shells after being incubated with PS NPs is ca. 5.2 μm similar to the template size. Given the fact that no efficient encapsulation for the PSS/PAH or PSS/PAH/ALG/PAH shells occurred, the compositions and properties of the shells, together with the charge density of the shell walls could be considered to be responsible for the effective encapsulation of NPs in the interior of the preformed shells.

ALG and CHI are two oppositely charged hydrophilic natural polysaccharides. Interestingly, the constructed (ALG/CHI)₅ shells in the phosphate buffer saline (PBS) solution have a diameter of 8.2 ± 0.3 μm (Fig. 5), which is remarkably larger than the template size (4.9 μm). The highly expanded shells of (ALG/CHI) are believed to be originated from the formation of the hydrogen bonds between two polysaccharides and the hydrogen bonds between the polysaccharides and water [18,21–24], which will inevitably cause the formation of a more porous scaffold with open porosity on the wall architecture that facilitates permeation of species with larger or rigid structures, for example, nanoparticles. Also, the expanded ALG/CHI shells are rather stable and have been verified to

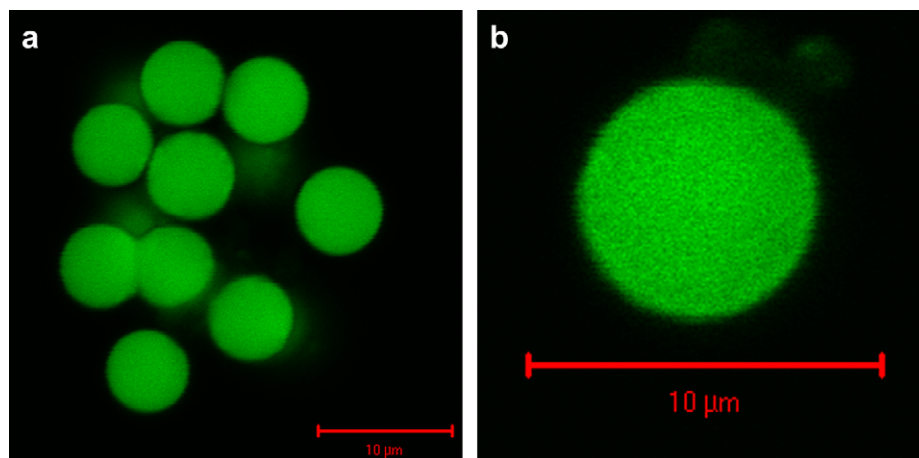


Fig. 3. (a) After the ALG/CHI shells were incubated in fluorescent-labeled PS NPs suspension, irreversible entrapment of NPs in the shells occurred; (b) magnified CLSM image of an individual PS NPs-loaded microshell.

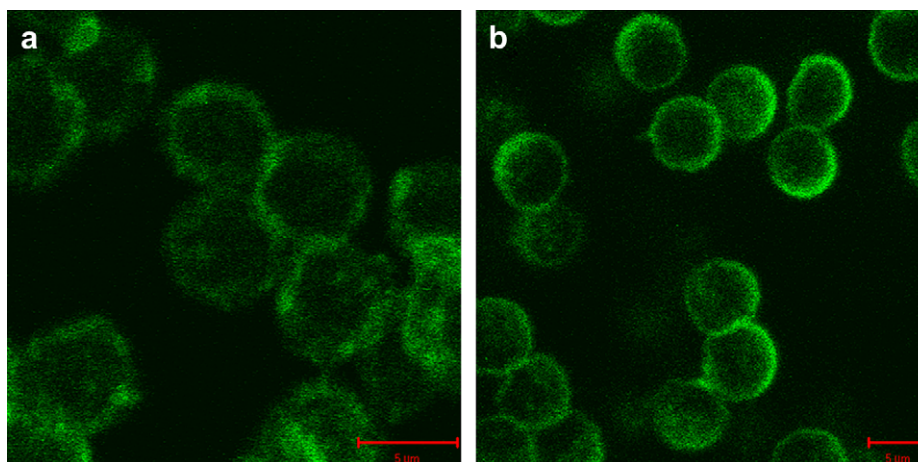


Fig. 4. CLSM images of hollow shells after being incubated with fluorescent-labeled PS NPs overnight: (a) (PSS/PAH)₅ and (b) (PSS/PAH)/(ALG/PAH)₄.

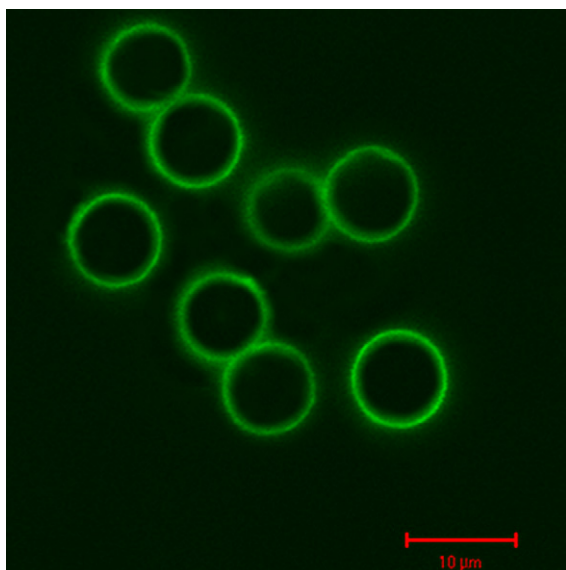


Fig. 5. CLSM image of hollow shells composed of (ALG/CHI)₅ templated onto 4.9 μm, where FITC-albumin was used to label the shells. Note: fluorescence intensity of the FITC-albumin from the interior of the shells was eliminated by reducing the mixture time of a fluorescence label reagent and a microshell suspension as well as rinsing with water.

possess good mechanical property based on the fact that the ALG/CHI shells can remain intact spherical structure in PSS solutions with different concentrations (upwards to 20.0 wt%) [18]. Apart from these, residual charges from shell walls might be considered as another important influence factor for the

effective encapsulation of NPs in the shells based on comparative study results, that is, NPs can enter into the ALG/CHI shells easily; while NPs are difficult to cross the layer barriers comprised of (PSS/PAH) or (PSS/PAH)/(ALG/PAH) due to the existence of more residual charges upon choosing PAH rather than CHI as a wall component (see Figs. 3 and 4).

Based on the above data and analysis, the encapsulation process of NPs in the shells of ALG and CHI is schematically outlined in Fig. 6. ALG and CHI both are natural and hydrophilic hydrogels. The as-prepared ALG/CHI microshells possess several particular advantages over the conventional synthesized microshells i.e. high swelling, elasticity and strong mechanical property. When the (ALG/CHI) shells were incubated in a nanoparticle suspension, several aspects of factors should be simultaneously considered for the efficient loading. (i) The highly expanded shells with enlarged holes on the wall texture are permeable to PS or SiO₂ NPs. Thus, NPs can cross the layer walls with low residual charges and enter into the shells due to the existence of a concentration gradient of NPs between the interior and exterior of the shells, and finally establish equilibrium between NPs suspended in the surrounding solution and within microshells. (ii) The network architecture of ALG/CHI shell walls is mechanically stable and shape-plastic, even upon loading relatively large rigid particles (280 nm SiO₂ and 260 nm PS used here). (iii) The loaded NPs might be more likely to exist in an aggregated or complex form so that the real concentration within the interior of the microshells is lower than in the bulk solution, thus promoting efficient encapsulation of NPs in the shells [10,18].

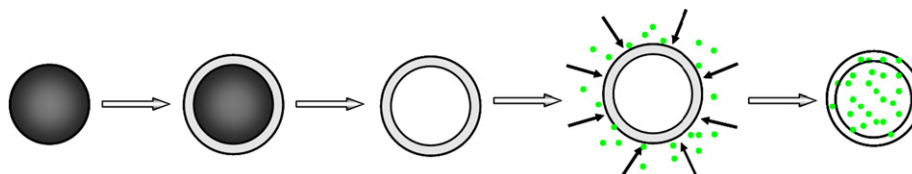


Fig. 6. Schematic illustration of the procedure for the encapsulation NPs in the LbL self-assembled ALG-CHI shells.

4. Conclusion

We have developed a facile method for encapsulation of nanoparticles in the bio-polyelectrolyte microshells. CLSM, TEM and SEM were employed to verify the efficient encapsulation of NPs in the shells. The encapsulation mechanism was also discussed. The hybrid NPs core/bio-polyelectrolyte shells might provide versatile applications as microcarriers in drug delivery and controlled release, optical materials as well as catalysis.

Acknowledgements

We gratefully acknowledge financial support from NSF of China (Nos. 20577002, 20546001, 50642042, and 20776014), the Key Program for Science and Technology Research from the ministry of education of China (No. 107009), the Program for New Century Excellent Talents in University (No. NCET-06-0102), and a startup scientific research fund for returned oversea scholars from the ministry of education of China.

References

- [1] (a) Iler RK. *J Colloid Interface Sci* 1966;21:569;
(b) Zhang X, Chen H, Zhang H. *Chem Commun* 2007:1395.
- [2] (a) Decher G. *Science* 1997;277:1232;
(b) Schmitt J, Decher G, Dressick WJ, Brandow SL, Geer RE, Shashidhar R, et al. *Adv Mater* 1997;9:61.
- [3] Keller SW, Johnson SA, Brigham ES, Yonemoto EH, Mallouk TE. *J Am Chem Soc* 1995;117:12879.
- [4] Ruths J, Essler F, Decher G, Riegler H. *Langmuir* 2000;16:8871.
- [5] Caruso F, Caruso R, Möhwald H. *Science* 1998;282:1111.
- [6] Peyratout CS, Dähne L. *Angew Chem Int Ed* 2004;43:3762.
- [7] Caruso F. *Colloids and colloid assemblies: synthesis, modification, organization and utilization of colloidal particles*. Weinheim: Wiley-VCH; 2003.
- [8] Ye S, Wang C, Liu X, Tong Z, Ren B, Zeng F. *J Controlled Release* 2006;112:79.
- [9] Gaponik N, Radtchenko IL, Gerstenberger MR, Fedutik YA, Sukhorukov BB, Rogach AL. *Nano Lett* 2003;3:369.
- [10] Zhu H, McShane M. *Langmuir* 2005;21:424.
- [11] Gao C, Möhwald H, Shen J. *ChemPhysChem* 2004;5:116.
- [12] Miyazaki S, Nakayama A, Oda M, Takada M, Attwood D. *Biol Pharm Bull* 1994;17:745.
- [13] Yan XL, Khor E, Lim LY. *J Biomed Mater Res* 2001;58:358.
- [14] Gaserod O, Sannes A, Skjak-Braek G. *Biomaterials* 1999;20:773.
- [15] Wang W, Liu X, Xie Y, Zhang H, Yu W, Xiong Y, et al. *J Mater Chem* 2006;16:3252.
- [16] Wang L, Khor E, Lim L-Y. *J Pharm Sci* 2001;90:1134.
- [17] El-Kamel A, Sokar M, Naggat V, Al Gamal S. *AAPS Pharm Sci* 2002;4 [Article 44].
- [18] Tao X, Sun X-J, Su J, Chen J-F, Roa W. *Polymer* 2006;47:6167.
- [19] Tao X, Su J, Chen J-F, Zhao J. *Chem Commun* 2005;12:4607.
- [20] Osses-Asare K, Arriagada FJ. *Colloids Surf* 1990;50:321–39.
- [21] Gao C, Leporatti S, Moya S, Donath E, Möhwald H. *Langmuir* 2001;17:3491.
- [22] Ravi Kumar MNV. *J Pharm Pharmaceut Sci* 2000;3:234.
- [23] Lee KY, Mooney DJ. *Chem Rev* 2001;101:1869.
- [24] Takeuchi H, Yasuji T, Yamamoto H, Kawashima Y. *Pharm Res* 2000;17:94.